

# Effect of Stochastic Gate Noise on Fault-Tolerant Surface Codes

Cherilyn Lee Gabriela Christen,  
Nathaniel James Pacey

In work under EPFL supervising Professor. Nicolas Macris

# Table of contents

**01.**

## **Stabilizer Code**

Fundamentals of quantum error correction

**02.**

## **Surface Code**

Error Detection Through Lattice-Based Syndromes

**03.**

## **Stochastic Noise**

Realistic Noise Implementation based on Noisy Quantum Gates

**04.**

## **Noise extension**

Custom Noise Extensions and Added Functionality

**05.**

## **Results**

Analysis of Custom Noise Implementation & Comparison to Qiskit Simulations

**06.**

## **Future Work**

Surface Code Extensions & Potential Noisy Gates Library Improvements



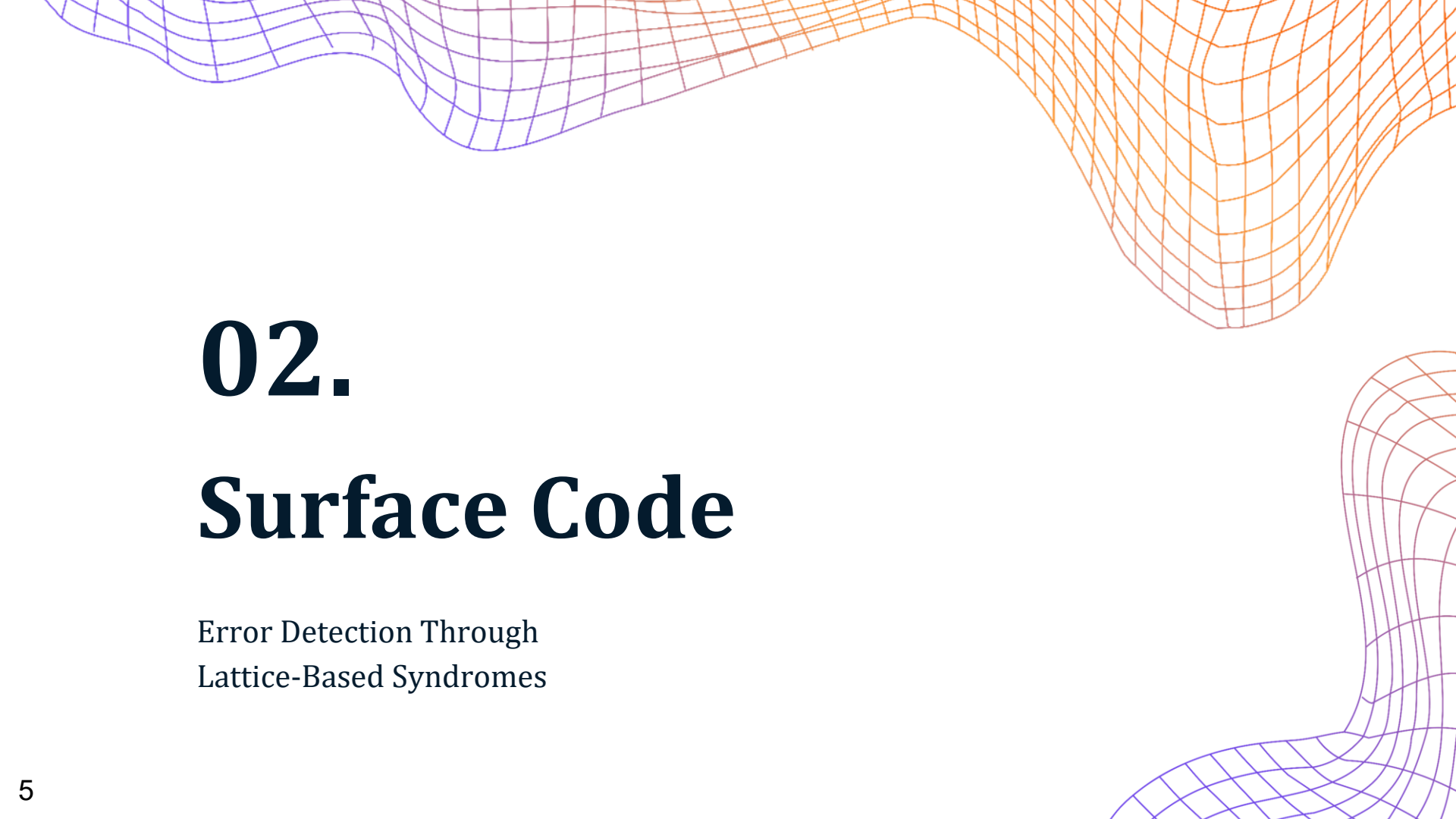
01.

# Stabilizer Code

Fundamentals of quantum  
error correction

# Stabilizer Code Basics

- A stabilizer code defines a subspace of the n-qubit Hilbert space using an abelian subgroup  $\mathcal{S} \subset \mathcal{P}_n$  of the Pauli group
- A codeword  $|\psi\rangle$  is any state stabilized by all  $S_i \in \mathcal{S}$ :  $S_i|\psi\rangle = |\psi\rangle$
- $\mathcal{S}$  has  $n-k$  independent generators; it encodes  $k$  logical qubits into  $n$  physical qubits  $\{S_1, S_2, \dots, S_{n-k}\} \subset \mathcal{P}_n$
- Logical operators commute with all  $S_i \in \mathcal{S}$ , but are not in  $\mathcal{S}$
- Error Detection:  $S_i(E|\psi\rangle) = \pm E S_i |\psi\rangle = \pm E |\psi\rangle$ 
  - If  $E$  commutes with  $S_i \rightarrow +1$ : error undetected
  - If  $E$  anti-commutes with  $S_i \rightarrow -1$ : error detected

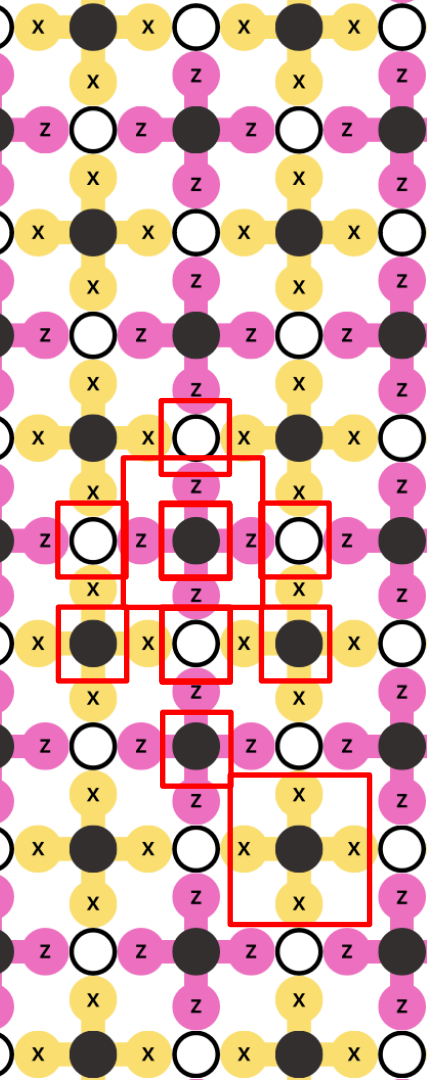


# 02. Surface Code

Error Detection Through  
Lattice-Based Syndromes

# Surface Code Structure

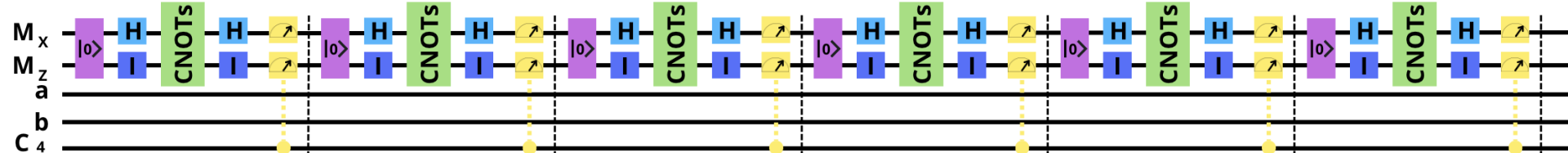
- Topological stabilizer code defined on a 2D lattice
- Data qubits encode quantum information
- Measurement (ancilla) qubits extract error syndromes
- Each measurement qubit:
  - Interacts with 4 neighboring data qubits
  - Implements measure-X (detects bit-flips) or measure-Z (detects phase-flips)
- Each data qubit connects to 2 measure-X and 2 measure-Z qubits
- Provides full single-qubit error coverage



\*Diagram based on: Surface codes: Towards practical large-scale quantum computation. [1]

# Surface Code Cycles

- Surface code operation proceeds in repeated measurement cycles
- After each cycle, the ancilla qubits are measured
- Once all stabilizer measurements are complete, the data qubits are projected into a state that simultaneously satisfies all measured eigenvalue constraints, this is known as the quiescent state
- These cycles are repeated, and in the absence of errors, the quiescent state remains stable due to the commutation of all stabilizers



# Surface Code Errors

- Focus on error detection rather than direct error correction
- Physical corrections are only applied if an error affects a measurement outcome; otherwise, errors are tracked in software
- Errors neutralize themselves when they reoccur in the same way since  $E^2 = I$  for  $E$  being any Pauli operator  $\{I,X,Y,Z\}$
- A Pauli-X error on the data qubit anticommutes with the Z-type stabilizer, and thus will be detected as a change in the corresponding measurement outcome
- A Pauli-Z error anticommutes with the X-type stabilizer and is similarly flagged by a measurement flip.

# 4 Qubit Example

Initial State of data qubits:  $|\psi\rangle_{a,b} = A|gg\rangle + B|ge\rangle + C|eg\rangle + D|ee\rangle$  with  $|A|^2 + |B|^2 + |C|^2 + |D|^2 = 1$

Initial State of all qubits:  $|\psi_0\rangle = |g\rangle \otimes |\psi\rangle_{a,b} \otimes |g\rangle = A|gggg\rangle + B|ggeg\rangle + C|gegg\rangle + D|geeg\rangle$

Apply the Hadamard gate to the X measurement qubit to change the basis:

$$|\psi_1\rangle = H_{M_x} I_{D_a} I_{D_b} I_{M_z} |\psi_0\rangle = (|g\rangle + |e\rangle) \otimes |\psi\rangle_{a,b} \otimes |g\rangle$$

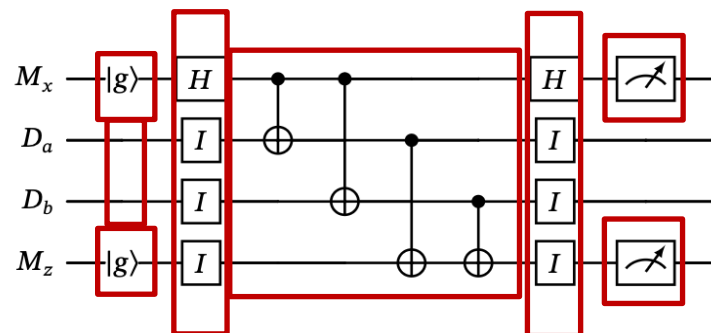
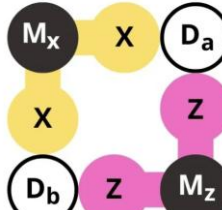
Apply the CNOT gates to create the entangled states :

$$\begin{aligned} |\psi_2\rangle &= CNOT_{M_x \rightarrow D_a} CNOT_{M_x \rightarrow D_b} CNOT_{D_a \rightarrow M_z} CNOT_{D_b \rightarrow M_z} |\psi_1\rangle \\ &= A(|gggg\rangle + |eeeg\rangle) + B(|ggee\rangle + |eege\rangle) + C(|gege\rangle + |egee\rangle) + D(|geeg\rangle + |eggg\rangle) \end{aligned}$$

Apply the Hadamard gate to the X measurement qubit to change the basis:

$$|\psi_3\rangle = H_{M_x} I_{D_a} I_{D_b} I_{M_z} |\psi_2\rangle$$

$$\begin{aligned} |\psi_3\rangle &= (A + D)(|g\rangle_{M_x} \otimes (|gg\rangle + |ee\rangle)_{D_a, D_b} \otimes |g\rangle_{M_z}) \\ &+ (B + C)(|g\rangle_{M_x} \otimes (|ge\rangle + |eg\rangle)_{D_a, D_b} \otimes |e\rangle_{M_z}) \\ &+ (A - D)(|e\rangle_{M_x} \otimes (|gg\rangle - |ee\rangle)_{D_a, D_b} \otimes |g\rangle_{M_z}) \\ &+ (B - C)(|e\rangle_{M_x} \otimes (|ge\rangle - |eg\rangle)_{D_a, D_b} \otimes |e\rangle_{M_z}) \end{aligned}$$



# Errors on 4 Qubit Example

The quiescent state was determined to be

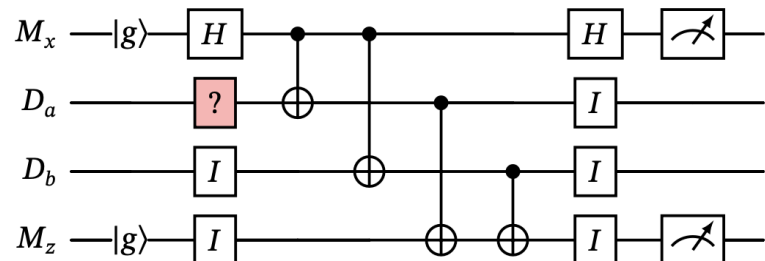
$|gg\rangle + |ee\rangle)_{D_a, D_b}$  in cycle 1

$$\begin{aligned} |\psi_3\rangle = & (A + D)(|g\rangle_{M_x} \otimes (|gg\rangle + |ee\rangle)_{D_a, D_b} \otimes |g\rangle_{M_z}) \\ & + (B + C)(|g\rangle_{M_x} \otimes (|ge\rangle + |eg\rangle)_{D_a, D_b} \otimes |e\rangle_{M_z}) \\ & + (A - D)(|e\rangle_{M_x} \otimes (|gg\rangle - |ee\rangle)_{D_a, D_b} \otimes |g\rangle_{M_z}) \\ & + (B - C)(|e\rangle_{M_x} \otimes (|ge\rangle - |eg\rangle)_{D_a, D_b} \otimes |e\rangle_{M_z}) \end{aligned}$$

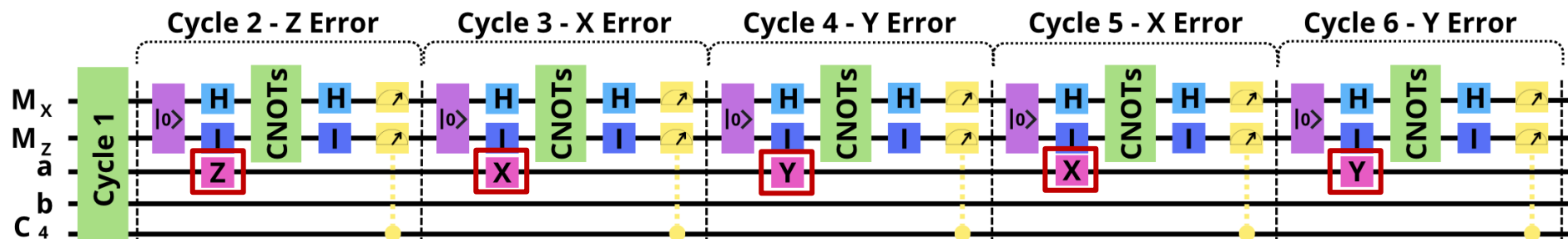
Having a X error on  $D_a$  in the next cycle results in a state  $|ge\rangle + |eg\rangle)_{D_a, D_b}$

$$\begin{aligned} |\psi_3\rangle = & (A + D)(|g\rangle_{M_x} \otimes (|gg\rangle + |ee\rangle)_{D_a, D_b} \otimes |g\rangle_{M_z}) \\ & + (B + C)(|g\rangle_{M_x} \otimes (|ge\rangle + |eg\rangle)_{D_a, D_b} \otimes |e\rangle_{M_z}) \\ & + (A - D)(|e\rangle_{M_x} \otimes (|gg\rangle - |ee\rangle)_{D_a, D_b} \otimes |g\rangle_{M_z}) \\ & + (B - C)(|e\rangle_{M_x} \otimes (|ge\rangle - |eg\rangle)_{D_a, D_b} \otimes |e\rangle_{M_z}) \end{aligned}$$

The measurement outcome is  $\{+1, -1\}$



# Errors on 4 - Qubit Example

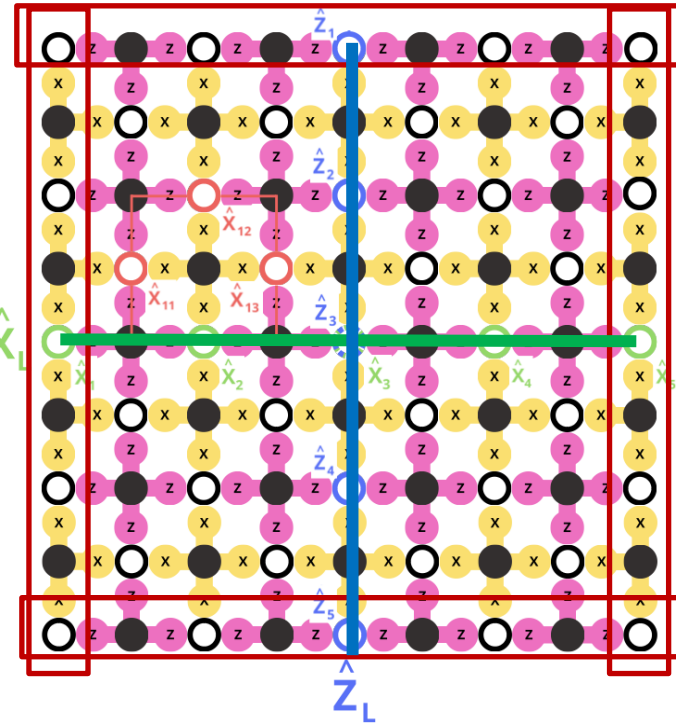


Single-shot stabilizer measurements



# Surface Code Logical Qubit

- A logical qubit in the surface code is defined using the degrees of freedom that remain after imposing all stabilizer constraints.
- Logical operators  $\hat{X}_L$  and  $\hat{Z}_L$  are constructed as products of single-qubit Pauli operators that commute with all stabilizers but are not themselves stabilizers.



\*Diagram based on: Surface codes: Towards practical large-scale quantum computation. [1]



# 9 Qubit Example

$$S_0 = X_a X_b X_c$$

$$S_1 = X_c X_d X_e$$

$$S_2 = Z_a Z_c Z_d$$

$$S_3 = Z_b Z_c Z_e$$

Since  $S_i|\psi\rangle = |\psi\rangle$ :

$$X_c X_d X_e |\psi\rangle = (+1) |\psi\rangle$$

$$Z_b Z_c Z_d |\psi\rangle = (+1) |\psi\rangle$$

$$X_a X_b X_c |\psi\rangle = (+1) |\psi\rangle$$

$$Z_a Z_c Z_d |\psi\rangle = (+1) |\psi\rangle$$

Experimentally it can be found that  
satisfy the above equations

$$|\psi\rangle = |ggggg\rangle + |eeegg\rangle + |ggeee\rangle + |eegee\rangle$$

$$|\psi'\rangle = |gwgge\rangle + |egege\rangle + |geeeg\rangle + |egwge\rangle$$

Defining the Logical Operators as

$$\hat{X}_L = X_b X_e$$

$$\hat{Z}_L = Z_d Z_e$$

$$[\hat{X}_L, S_i] = 0$$

$$[\hat{Z}_L, S_i] = 0$$

one can see that

$$\hat{X}_L |\psi\rangle = |\psi'\rangle$$

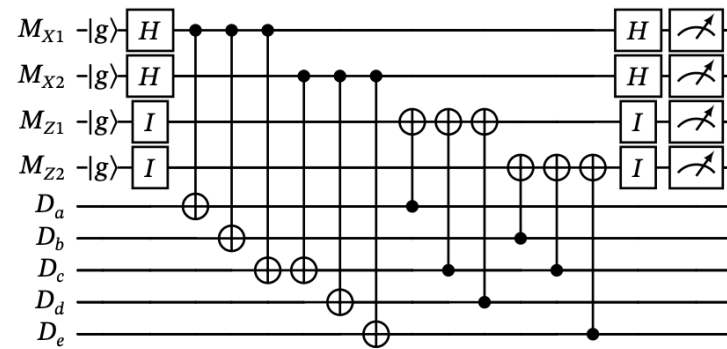
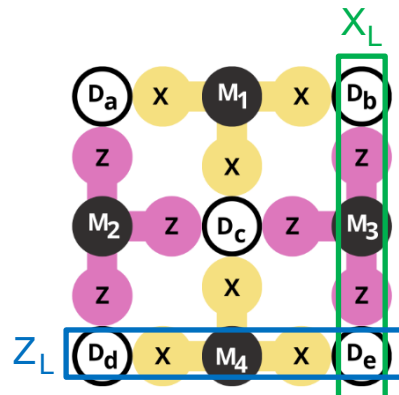
$$\hat{X}_L |\psi'\rangle = |\psi\rangle$$

$$\hat{Z}_L |\psi\rangle = |\psi\rangle$$

$$\hat{Z}_L |\psi'\rangle = -|\psi'\rangle$$

$$|\psi\rangle = |0\rangle_L$$

$$|\psi'\rangle = |1\rangle_L$$

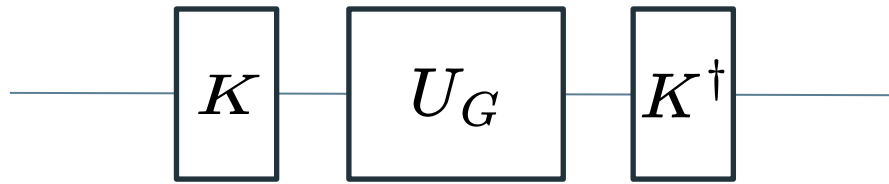


# 03.

# Stochastic Noise

Realistic Noise Implementation based  
on *Noisy Quantum Gates*

# Traditional Noise



# Lindblad Formalism

Lindblad formalism describes the non-unitary dynamics of open quantum systems under Markovian decoherence

Lindblad-type master equation:

$$\frac{d\rho}{dt} = -\frac{i}{\hbar} [H, \rho] + \sum_k \left( L_k \rho L_k^\dagger - \frac{1}{2} \{ L_k^\dagger L_k, \rho \} \right)$$

Itô stochastic differential equation for the state evolution:

$$d|\psi_s\rangle = \left[ -\frac{i}{\hbar} H_s ds + \sum_{k=1}^{N^2-1} \left( i\epsilon dW_{k,s} L_k - \frac{\epsilon^2}{2} ds L_k^\dagger L_k \right) \right] |\psi_s\rangle$$

Transforming this into the interaction picture:

$$d|\phi_s\rangle = \left[ i\epsilon \sum_k dW_{k,s} L_{k,s} - \frac{\epsilon^2}{2} \sum_k ds L_{k,s}^\dagger L_{k,s} \right] |\phi_s\rangle.$$

$$L_{k,s} = L_k(s) = U_s^\dagger \sigma_k U_s$$

\*Equations from: Noisy gates for simulating quantum computers [2].

# Noisy Gate

$$N_g = U_g e^{\Lambda} e^{\tilde{\Xi}}$$

Deterministic term  $\Lambda = -\frac{\epsilon^2}{2} \int_0^1 ds \sum_{k=1}^{N^2-1} [L_{k,s}^\dagger L_{k,s} - L_{k,s}^2]$

Stochastic term 
$$\left\{ \begin{array}{l} \tilde{\Xi} = i\epsilon \sum_{k=1}^{N^2-1} \int_0^1 dW_{k,s} L_{k,s} + \mathcal{C} \\ \mathcal{C} = -\frac{\epsilon^2}{2} \sum_{k,l=1}^{N^2-1} \int_0^1 dW_{k,s} \int_0^s dW_{l,s'} [L_{k,s}, L_{l,s'}] \end{array} \right.$$

(full derivation in report)

$$L_{k,s} = L_k(s) = U_s^\dagger \sigma_k U_s$$

\*Equations from: Noisy gates for simulating quantum computers [2].

# Noisy Gates Single Qubit Noise

$$U(\theta, \phi) = \exp(-i\theta R_{xy}(\phi)/2)$$

$$R_{xy}(\phi) = \cos(\phi)X + \sin(\phi)Y$$

$$H(\theta, \phi) = \frac{\theta \hbar}{2} R_{xy}(\phi)$$

# Depolarizing Noise

Lindblad operator  $L_{k,s}$  as a linear combination of the Pauli basis  $\{\mathbb{I}, X, Y, Z\}$

$$L_{k,s} = U_s^\dagger \sigma_k U_s$$

$$L_{k,s} = f_{k,s}^{(I)} \mathbb{I} + f_{k,s}^{(X)} X + f_{k,s}^{(Y)} Y + f_{k,s}^{(Z)} Z = \left( \sum_{j=0}^3 f_k^{(j)}(s) \sigma_j \right)$$

$$f_{k,s}^{(i)} = \frac{1}{2} \text{Tr} [L_{k,s} \cdot \sigma_i]$$

For the depolarizing channel specifically, the noise model is described by three time-dependent Lindblad operators:

$$L_{X,s}^{(\text{dep})} = \sqrt{\frac{p}{4}} X(s), \quad L_{Y,s}^{(\text{dep})} = \sqrt{\frac{p}{4}} Y(s), \quad L_{Z,s}^{(\text{dep})} = \sqrt{\frac{p}{4}} Z(s) \quad p \text{ is the depolarizing probability}$$

$$\epsilon_d = \sqrt{\frac{p}{4}}$$

Substituting  $L_{k,s}$  into  $\Xi = i\epsilon \sum_{k=1}^{N^2-1} \int_0^1 dW_{k,s} L_{k,s}$ :

$$\Xi = i\epsilon_d \sum_{j=1}^3 \sum_k \left( \int_0^1 f_k^{(j)}(s) dW_{k,s} \right) \sigma_j$$

# Depolarizing Noise

Define a real stochastic variable  $\xi_k^{(j)}$  such that  $\xi_k^{(j)} := \int_0^1 f_k^{(j)}(s) dW_{k,s} \rightarrow \Xi = i \epsilon_d \sum_{j=1}^3 \sum_k \xi_k^{(j)} \sigma_j$

To fully characterize the distribution of  $\Xi$ , we compute the covariance matrix  $\boldsymbol{\xi} = (\xi_x, \xi_y, \xi_z)$

The covariance matrix  $\Sigma_k^{(ij)}$  expands to

$$\Sigma_k^{(ij)} = \mathbb{E}[\xi_k^{(i)} \xi_k^{(j)}] \rightarrow \Sigma_k^{(ij)} = \int_0^1 f_k^{(i)}(s) f_k^{(j)}(s) ds$$

The full stochastic noise term  $\Xi$  is constructed by decomposing it into contributions  $\Xi_X$ ,  $\Xi_Y$ , and  $\Xi_Z$  associated with each Pauli direction

$$\Xi = \sum_k \Xi_k \quad \begin{aligned} U_s^\dagger X U_s &= f_X^{(I)}(s) I + f_X^{(x)}(s) X + f_X^{(y)}(s) Y + f_X^{(z)}(s) Z \\ U_s^\dagger Y U_s &= f_Y^{(I)}(s) I + f_Y^{(x)}(s) X + f_Y^{(y)}(s) Y + f_Y^{(z)}(s) Z \\ U_s^\dagger Z U_s &= f_Z^{(I)}(s) I + f_Z^{(x)}(s) X + f_Z^{(y)}(s) Y + f_Z^{(z)}(s) Z \end{aligned}$$

(A full derivation and several examples are in the report)

# Additional Noise

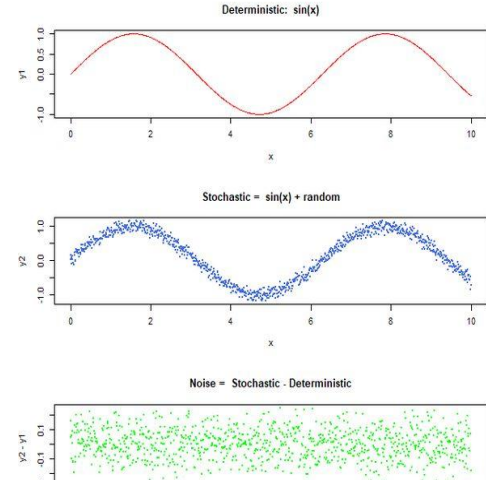
## Stochastic noise:

- Depolarizing  $\Xi = i \epsilon_d \sum_{j=1}^3 \sum_k \xi_k^{(j)} \sigma_j$
- Amplitude Damping  $L_{\downarrow,s}^{(\text{ad})} = \sqrt{\frac{1}{T_1}} \sigma_-(s) \quad \mathbf{I}_r = \epsilon_1 \begin{pmatrix} -\frac{i}{2} e^{i\phi} I_r^{(2)} & I_r^{(1)} - I_r^{(3)} \\ e^{2i\phi} I_r^{(3)} & \frac{i}{2} e^{i\phi} I_r^{(2)} \end{pmatrix}$
- Phase Damping  $L_{Z,s}^{(\phi)} = \sqrt{\frac{1}{T_1}} Z(s) \quad \mathbf{I}_p = \epsilon_\phi \begin{pmatrix} I_p^{(1)} & -i e^{-i\phi} I_p^{(2)} \\ i e^{i\phi} I_p^{(2)} & -I_p^{(1)} \end{pmatrix}$

## Deterministic Noise

$$\Lambda = -\frac{\epsilon^2}{2} \int_0^1 ds \sum_{k=1}^{N^2-1} [L_{k,s}^\dagger L_{k,s} - L_{k,s}^2]$$

$$\Lambda = -\frac{\epsilon_1^2}{2} \begin{pmatrix} \det_1 & \frac{i}{2} e^{-i\phi} \det_2 \\ -\frac{i}{2} e^{i\phi} \det_2 & \det_3 \end{pmatrix}$$



\*Source: Paweł Cisło, Industrial Engineering  
Type of Model (Deterministic, Stochastic, Noise)

# 04.

## Noise Extension

Beyond Noisy-Gates: Custom Noise  
Extensions and Added Functionality

# Noise Extensions

Apply noise to each type of 1-qubit gate individually

$$U_s = e^{-is\theta R_{xyz}(\phi, \psi)}$$

$$R_{xyz}(\phi, \psi) = \cos(\phi) \sin(\psi) X + \sin(\phi) \sin(\psi) Y + \cos(\psi) Z$$

Pauli Basis Components  $f_Y^{(j)}(s)$  for  $R_{xyz}$  Rotation

$$f_Y^{(I)}(s) = 0$$

$$f_Y^{(x)}(s) = \sin(2\phi) \sin^2(\psi) \sin^2\left(\frac{s\theta}{2}\right) + \sin(s\theta) \cos(\psi)$$

$$f_Y^{(y)}(s) = -\sin^2(\psi) \sin^2\left(\frac{s\theta}{2}\right) \cos(2\phi) - \sin^2\left(\frac{s\theta}{2}\right) \cos^2(\psi) + \cos^2\left(\frac{s\theta}{2}\right)$$

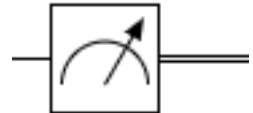
$$f_Y^{(z)}(s) = 2 \left( \sin(\phi) \sin\left(\frac{s\theta}{2}\right) \cos(\psi) - \cos(\phi) \cos\left(\frac{s\theta}{2}\right) \right) \sin(\psi) \sin\left(\frac{s\theta}{2}\right)$$

Gate	$\theta$	$\psi$	$\phi$
$I$	$2\pi$	-	-
$X$	-	$\frac{\pi}{2}$	0
$Y$	-	$\frac{\pi}{2}$	$\frac{\pi}{2}$
$Z$	-	0	$\frac{\pi}{2}$

$$\Sigma_Y^{(x)} = \begin{pmatrix} \frac{2\theta + \sin(2\theta)}{4\theta} & 0 & \frac{\sin^2(\theta)}{2\theta} \\ 0 & 0 & 0 \\ \frac{\sin^2(\theta)}{2\theta} & 0 & \frac{2\theta - \sin(2\theta)}{4\theta} \end{pmatrix}$$

$$\Sigma_k^{(ij)} = \mathbb{E}[\xi_k^{(i)} \xi_k^{(j)}] \rightarrow \Sigma_k^{(ij)} = \int_0^1 f_k^{(i)}(s) f_k^{(j)}(s) ds$$

# Measurement Implementation



Custom measurement routine in QuTiP. For an  $N$ -qubit state  $|\psi\rangle$  and a target qubit  $i$ , the code constructs the projectors:

$$P_1^{(i)} = (I_2)^{\otimes i} \otimes |1\rangle\langle 1| \otimes (I_2)^{\otimes(N-i-1)}$$

$$P_0^{(i)} = \underbrace{(I_2)^{\otimes i}}_{\text{qubits } 0\dots i-1} \otimes |0\rangle\langle 0| \otimes \underbrace{(I_2)^{\otimes(N-i-1)}}_{\text{qubits } i+1\dots N-1}$$

The Born-rule probabilities are then evaluated as

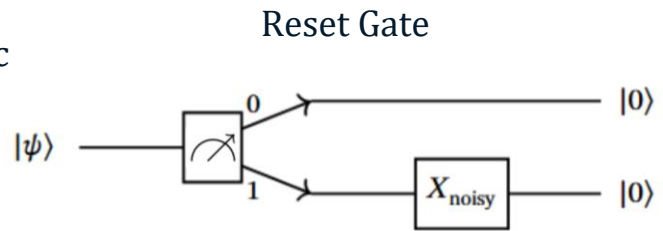
$$p_0 = \langle\psi|P_0^{(i)}|\psi\rangle, \quad p_1 = \langle\psi|P_1^{(i)}|\psi\rangle, \quad p_0 + p_1 = 1$$

Measurement outcome  $k \in \{0, 1\}$  is randomly sampled with probabilities  $\{p_0, p_1\}$ ; the collapsed state is projected onto  $P_k^{(i)}$  and re-normalized.

$$|\psi_{out}\rangle = \frac{P_k^{(i)}|\psi\rangle}{\sqrt{\langle\psi|P_k^{(i)}|\psi\rangle}}$$

# Noisy Reset Gate Implementation

- The *noisy-gates* library lacks native support for noisy resets resets critical for surface code cycles.
- A custom noisy reset was implemented to simulate realistic error conditions.
- **Approach:**
  - Perform a projective measurement on the qubit.
  - If outcome is  $|1\rangle$ , apply a noisy  $X$  gate to reset to  $|0\rangle$ .
  - Otherwise return  $|\psi\rangle$ .
- Enables repeated stabilizer cycles with more physically accurate reset behavior.

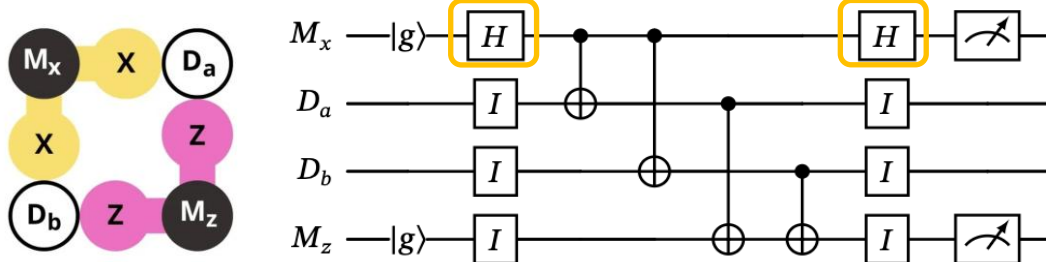


# Noisy Hadamard Gate Implementation

- Our framework applies noise individually to each gate
- Only 1-qubit gates are Reset and Hadamard
- We construct the noisy Hadamard gate, by combining the noisy  $X$  and  $Z$  gates.

$$H = \frac{1}{\sqrt{2}} \begin{bmatrix} 1 & 1 \\ 1 & -1 \end{bmatrix}$$

$$H_{\text{noisy}} = \frac{1}{\sqrt{2}} (X_{\text{noisy}} + Z_{\text{noisy}})$$

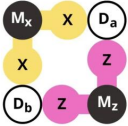




# 05. Results

Analysis of Custom Noise  
Implementation &  
Comparison to Qiskit Simulations

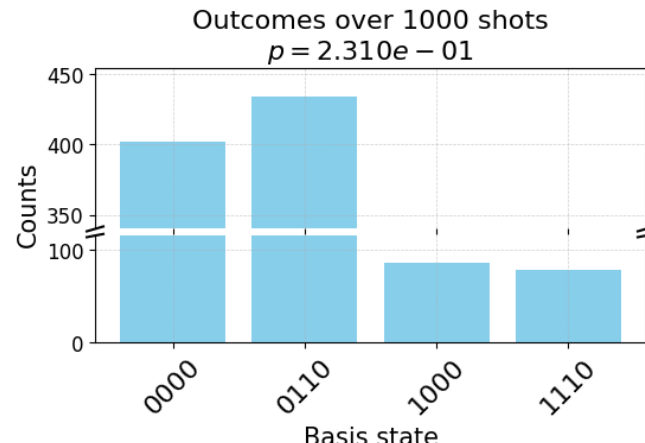
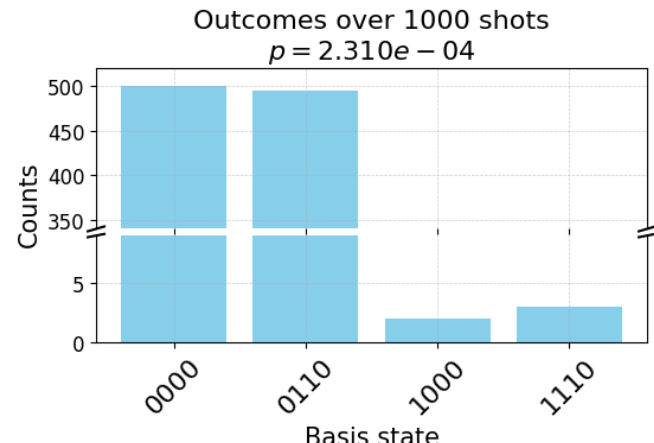
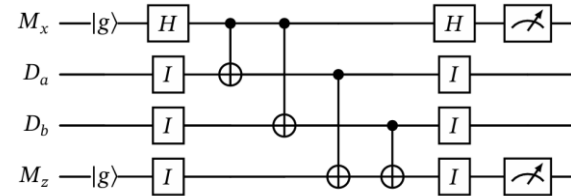
# Analysis of Custom Noise Implementation

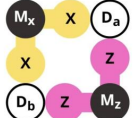


Effect of Noise Model over on Measurement Outcomes

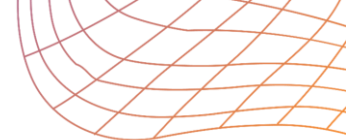
$$|\Phi^+\rangle_{D_a, D_b} = \frac{1}{\sqrt{2}}(|00\rangle + |11\rangle)_{D_a, D_b}$$

$$|\psi_{\text{in}}\rangle = |0\rangle_{M_x} \otimes |\Phi^+\rangle_{D_a, D_b} \otimes |0\rangle_{M_z}$$





# Analysis of Custom Noise Implementation



## Single-Cycle Surface Code Behavior Under Varying Noise

Generally: for a non-noisy mixed state

$$\rho = \sum_k p_k |\psi_k\rangle\langle\psi_k|, \quad \text{with} \quad \sum_k p_k = 1,$$

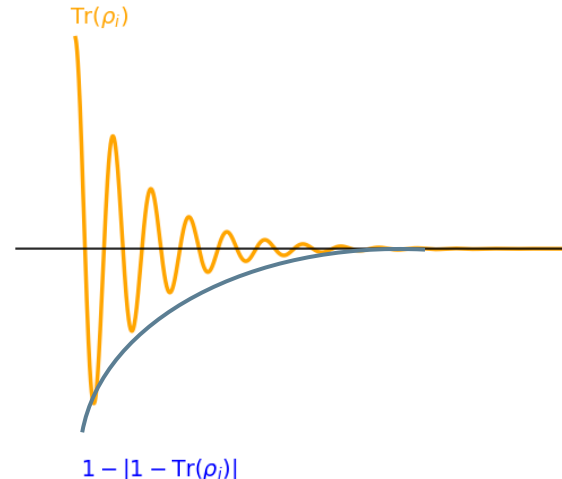
$$\text{Tr}(\rho) = \sum_k p_k \text{Tr}(|\psi_k\rangle\langle\psi_k|) = \sum_k p_k \langle\psi_k|\psi_k\rangle = \sum_k p_k = 1$$

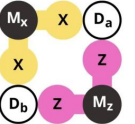
But for a noisy state

$$\text{Tr}(\rho_{noisy}) = \|\psi_{noisy}\|^2 \neq 1$$

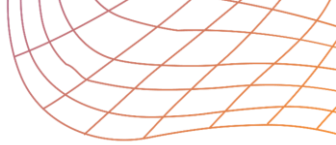
But stochastic noise is trace-preserving in expectation

$$\langle \text{Tr}(\rho_i) \rangle \rightarrow 1$$

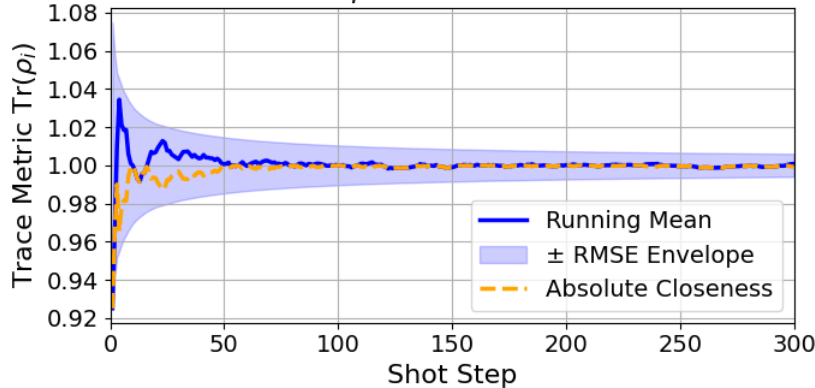




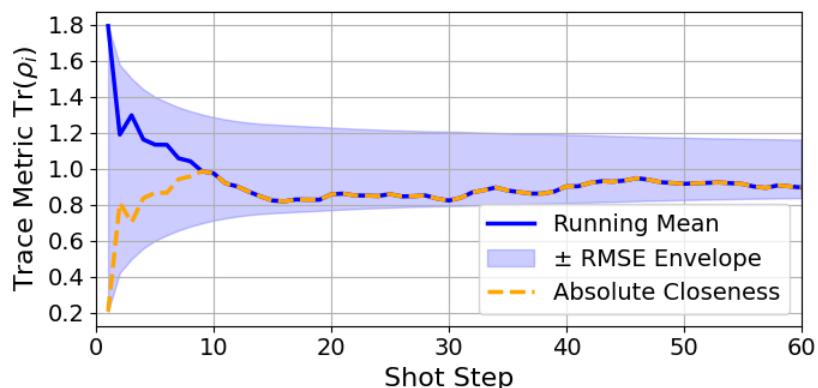
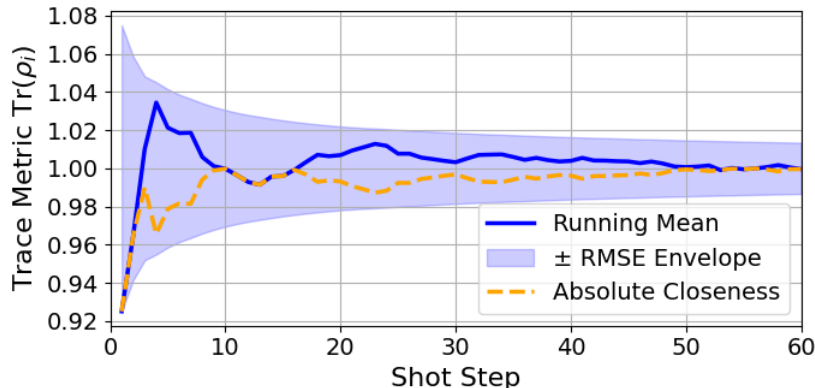
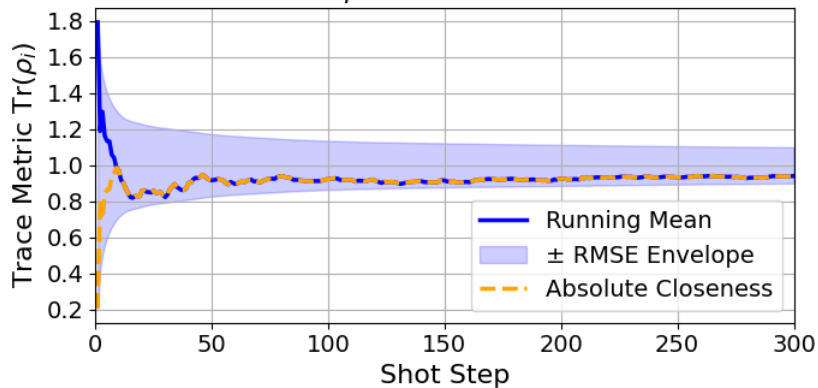
# Analysis of Custom Noise Implementation

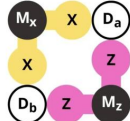


Convergence of  $\text{Tr}(\rho_i)$  to Unity with RMSE Envelope  
 $p = 2.310e - 04$

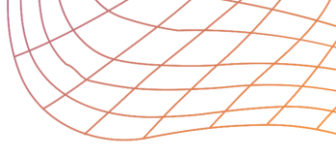


Convergence of  $\text{Tr}(\rho_i)$  to Unity with RMSE Envelope  
 $p = 2.310e - 01$





# Analysis of Custom Noise Implementation



## Fidelity Metric

To quantify closeness, we compute the fidelity

$$\mathcal{F}(\rho_i, \rho_{\text{ideal}}) = \left( \text{Tr} \sqrt{\sqrt{\rho_{\text{ideal}}} \rho_i \sqrt{\rho_{\text{ideal}}}} \right)^2$$

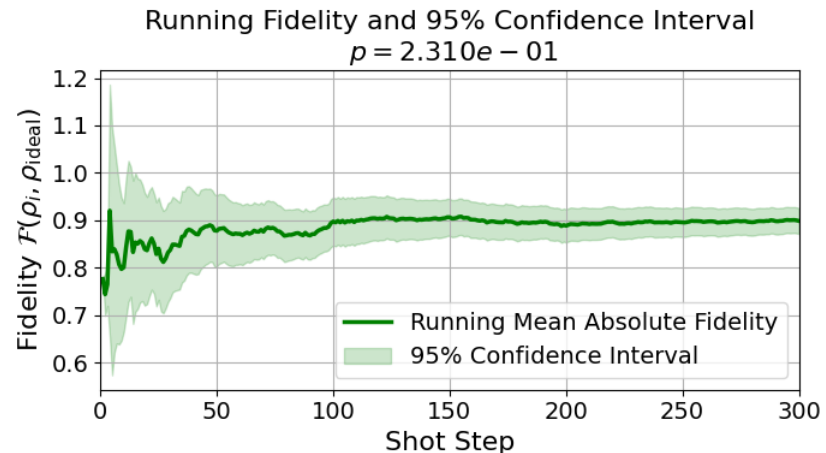
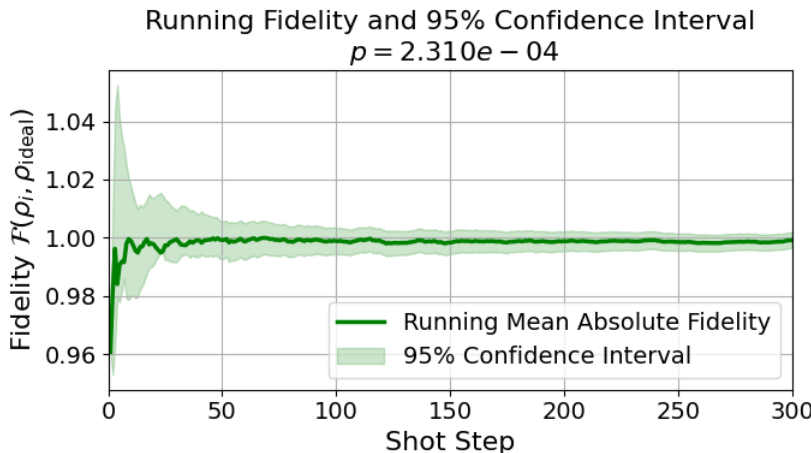
## Running Mean Fidelity

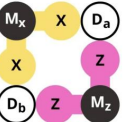
To observe convergence over repeated shots

$$\langle \mathcal{F} \rangle_n = \frac{1}{n} \sum_{i=1}^n \mathcal{F}(\rho_i, \rho_{\text{ideal}})$$

## Closeness to Perfect Fidelity

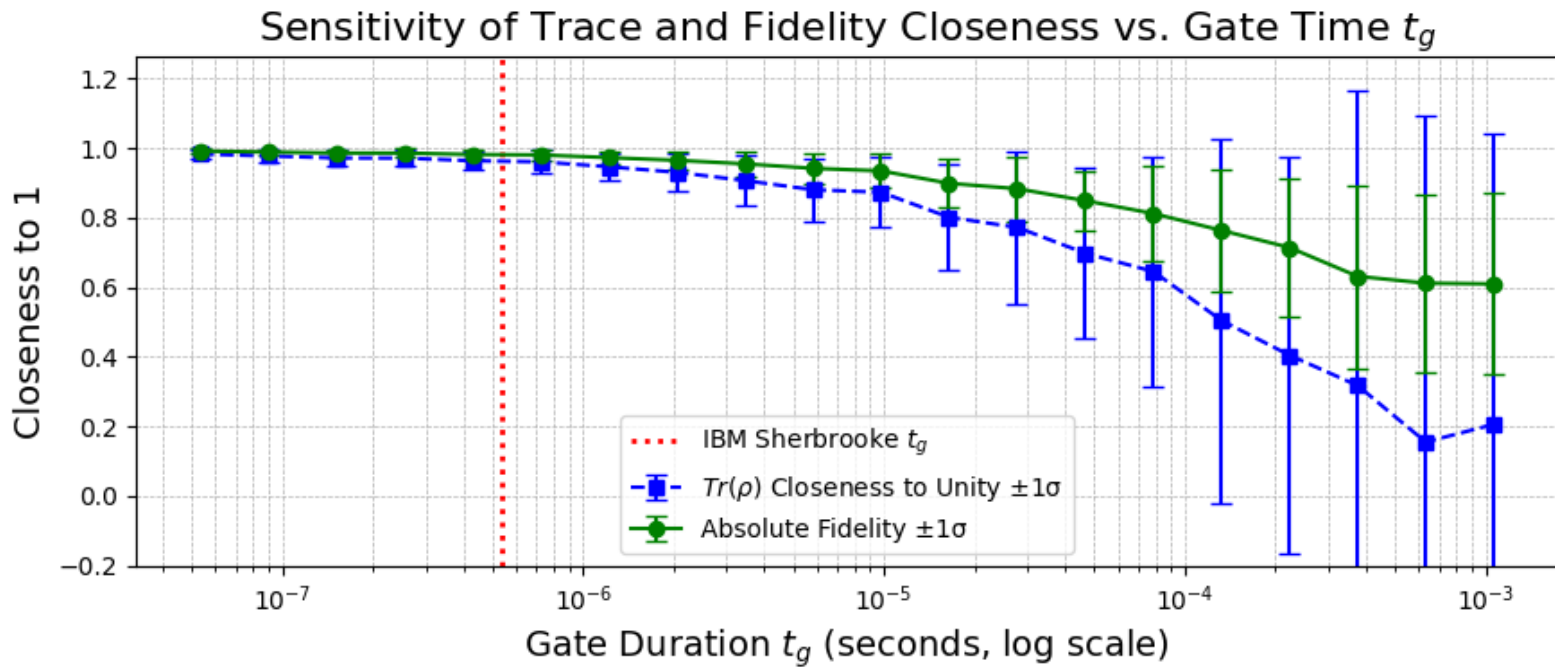
$$1 - |\langle \mathcal{F} \rangle_n - 1|$$

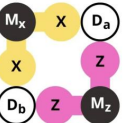




# Sensitivity of Error Metrics to Device Parameters

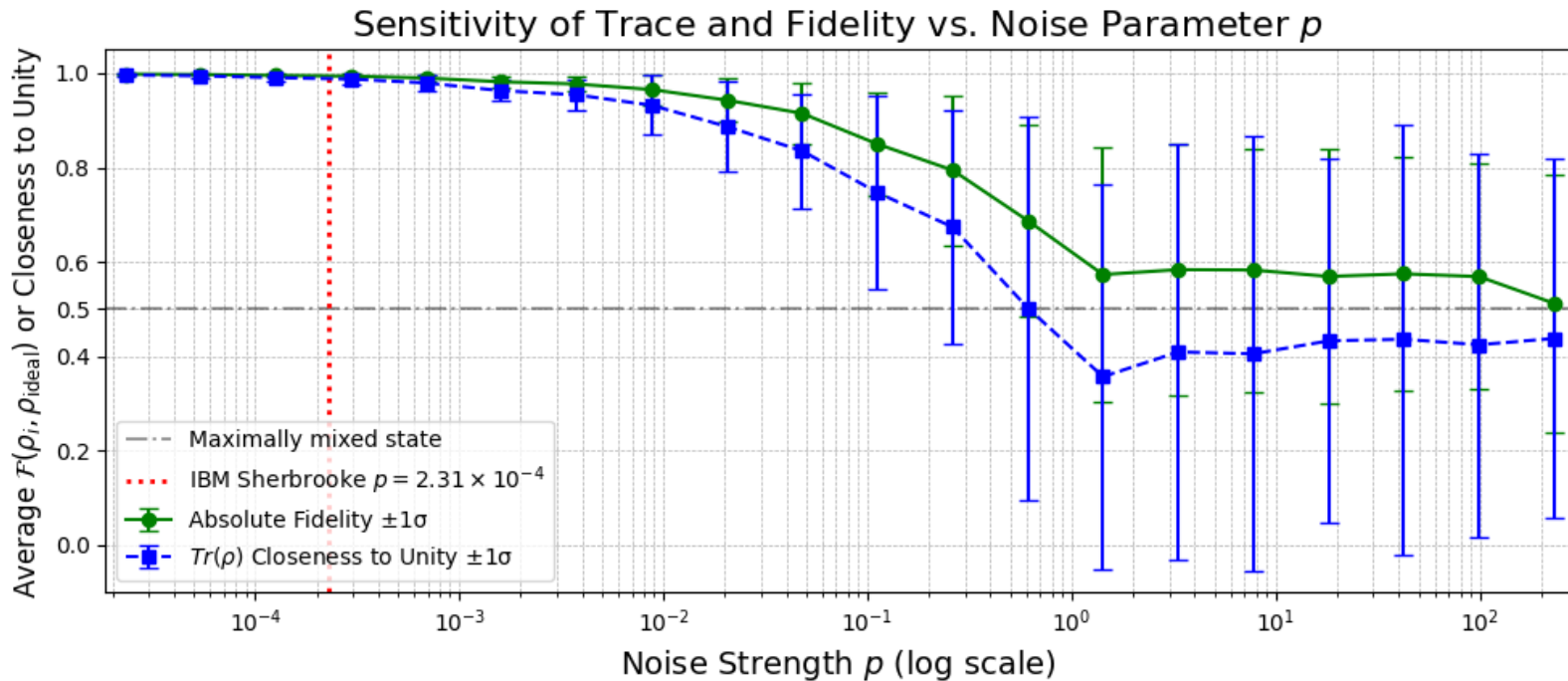
Stochastic noise increases with gate duration due to time-integrated decoherence from Lindblad dynamics.

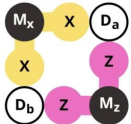




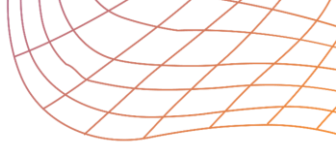
# Sensitivity of Error Metrics to Device Parameters

Increasing depolarizing noise strength leads to lower fidelity and greater trace deviation due to enhanced randomization of the quantum state.

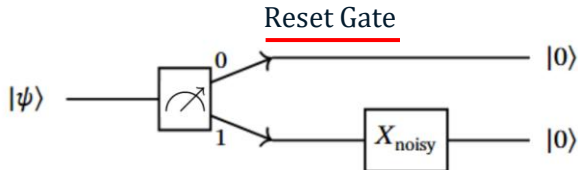
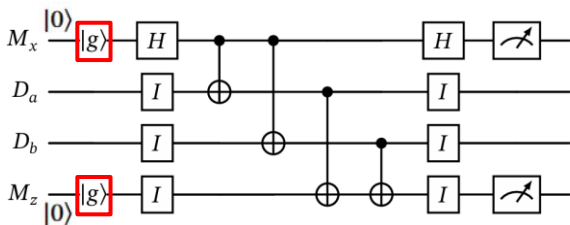
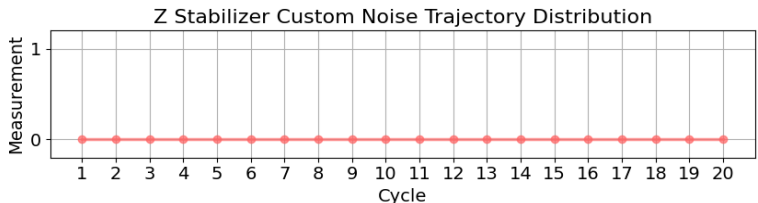
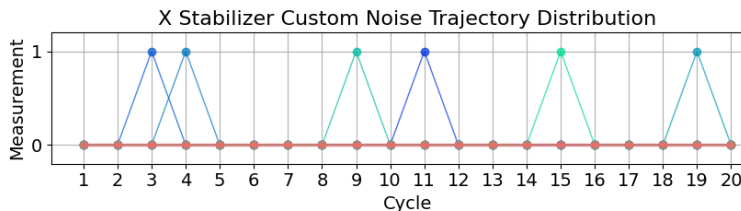
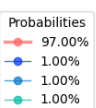
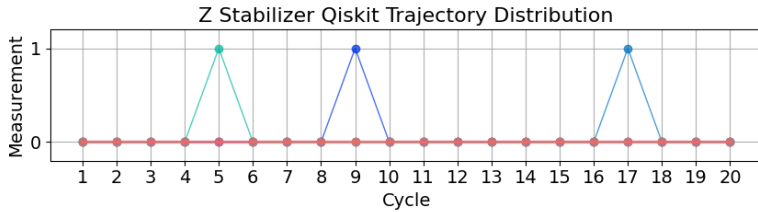
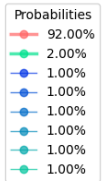
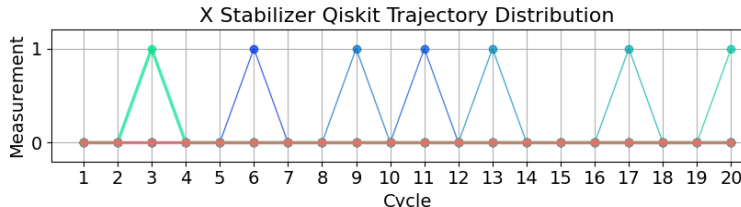


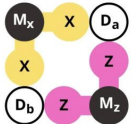


# Comparison to Qiskit Noise Simulation



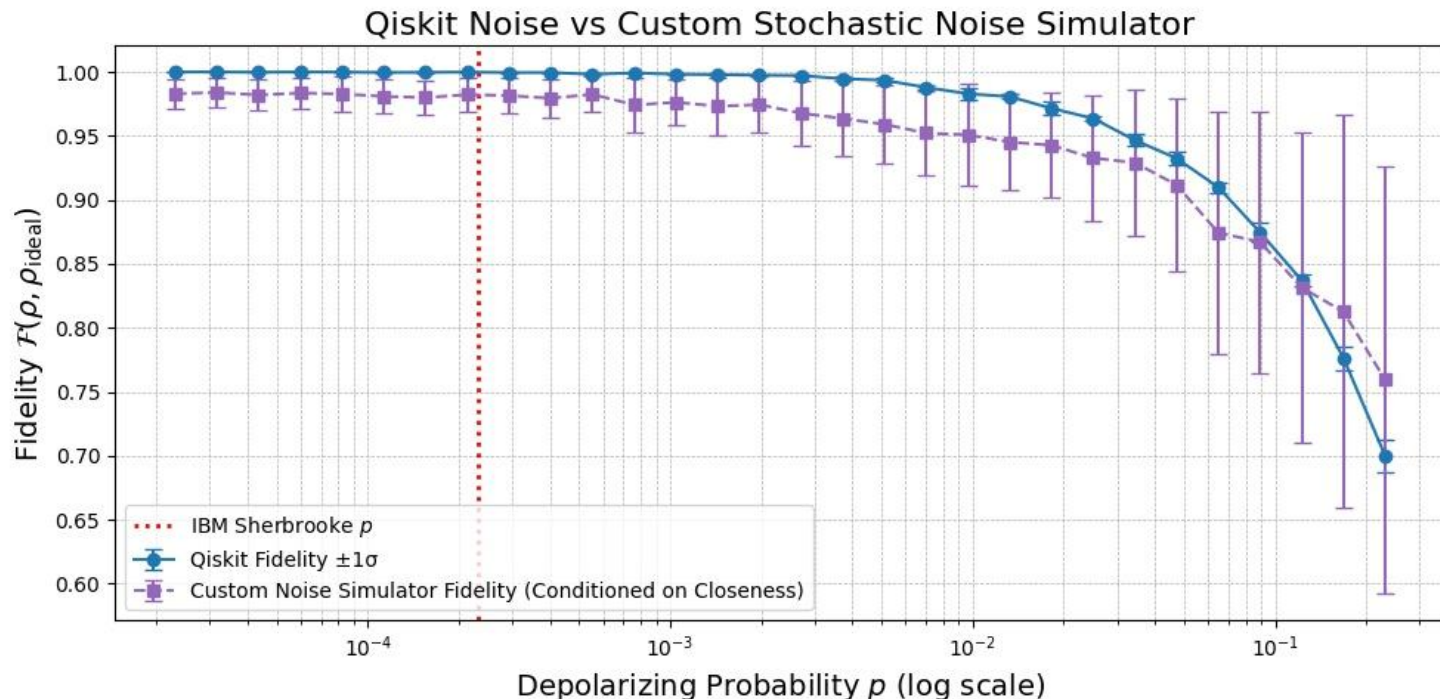
Effects of noise model over many surface code cycles' trajectory

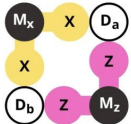




# Comparison to Qiskit Noise Simulation

Comparison of absolute fidelity of Qiskit noise model and stochastic noise model over a range of depolarizing noise strengths.



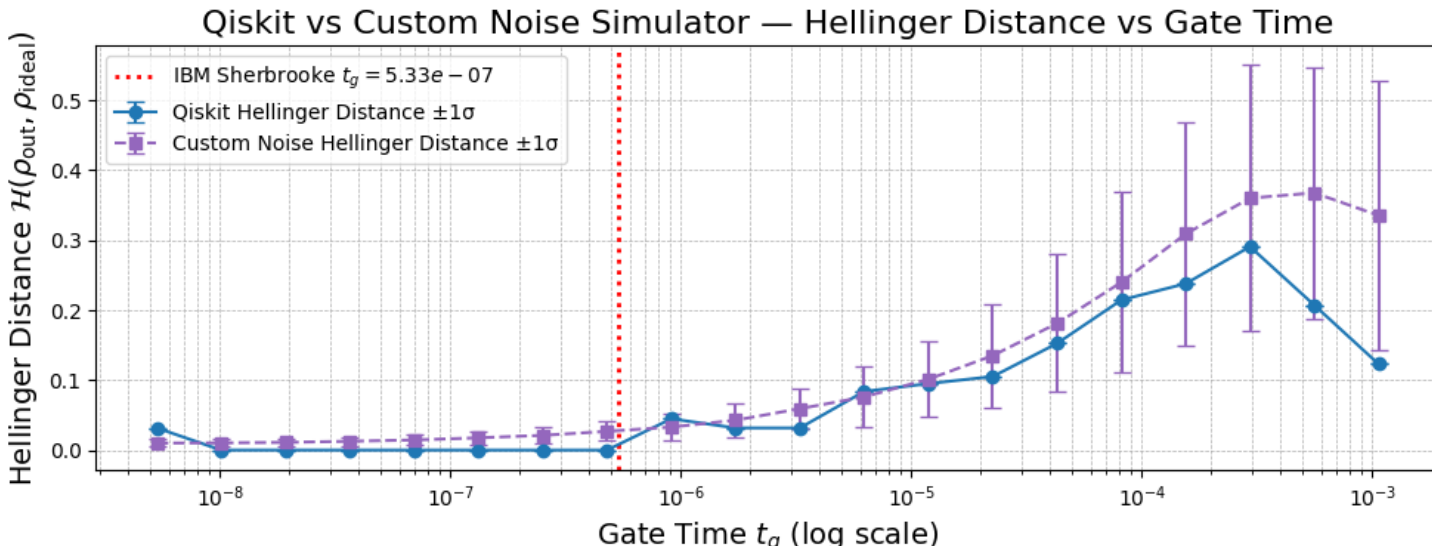


# Comparison to Qiskit Noise Simulation

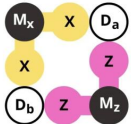


Hellinger distance focuses on differences in measurement statistics, making it particularly useful for evaluating the practical impact of noise on observable outcomes\*

$$\mathcal{H}(\rho, \sigma) = \frac{1}{\sqrt{2}} \sqrt{\sum_{k=1}^N (\sqrt{\rho_{kk}} - \sqrt{\sigma_{kk}})^2}$$



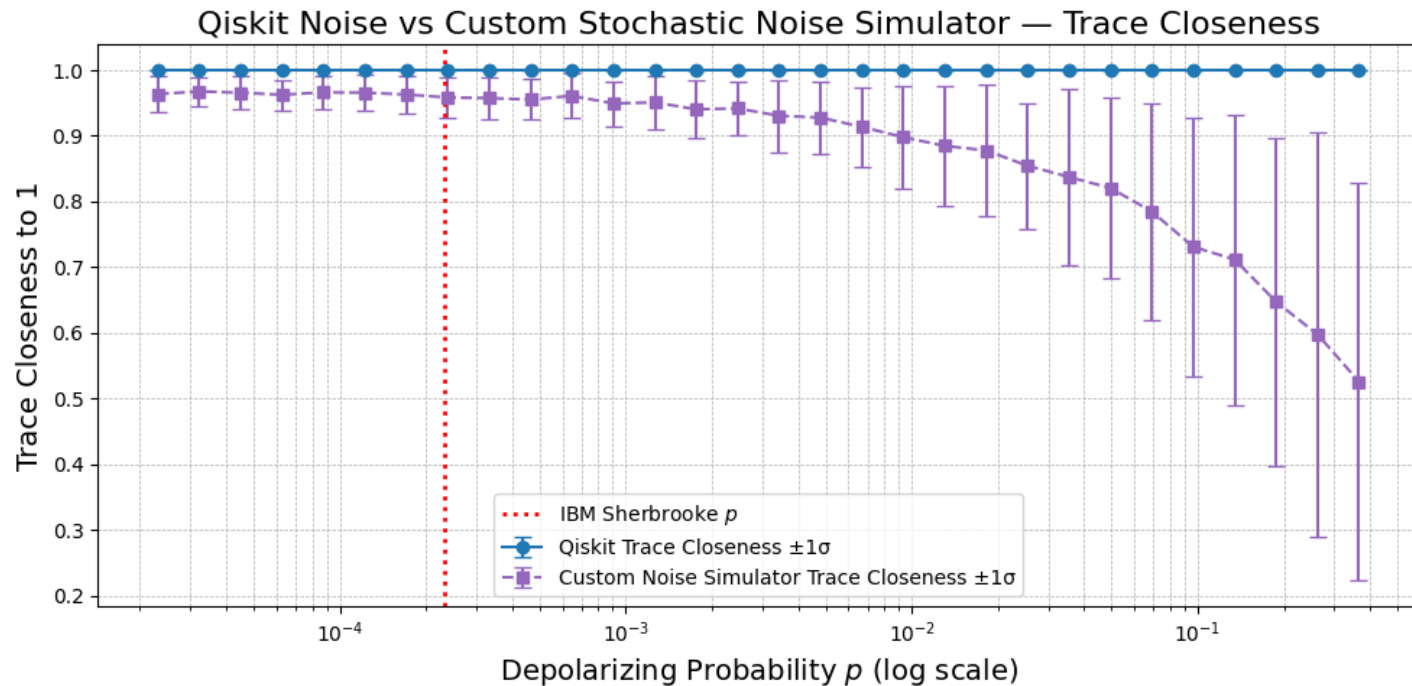
\*Equations from: Noisy gates for simulating quantum computers.[2]



# Comparison to Qiskit Noise Simulation



Stochastic model evolves from an absolute  $\text{Tr}(\rho)$  near unity toward 0.5, the value expected for a maximally mixed state, while the Qiskit trace remains fixed at 1

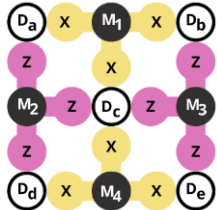


# 06.

## Future Work

Surface Code Extensions &  
Potential Noisy Gates Library  
Improvements

# Surface Code Extensions



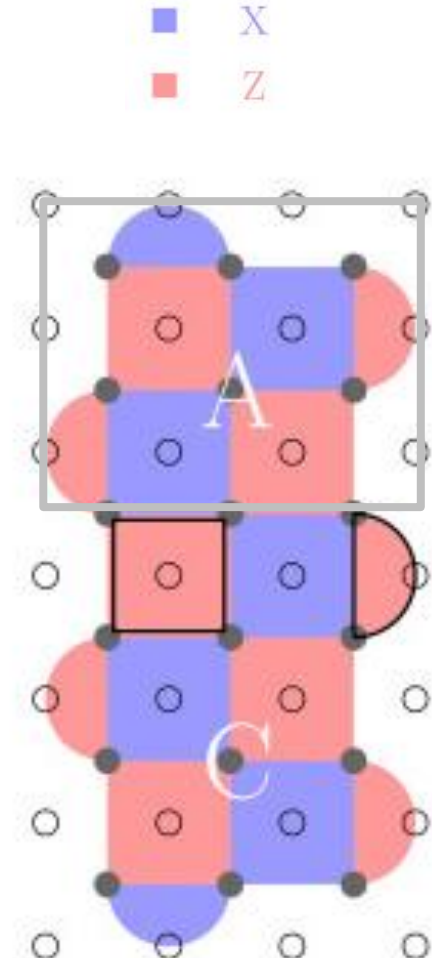
Distance-3 surface code requires:

- 17 qubits (rotated layout) or
- 25 qubits (non-rotated layout) for full single-qubit error protection.

**Goal:** Implement physically motivated two-qubit noise models for full logical qubit simulation.

Syndrome decoding to use MWPM for error correction.

**Future benchmark:** Compare noisy surface code simulation with real IBM Quantum hardware implementation.



\*Figure from: Mapping of lattice surgery-based quantum circuits on surface code architectures [9].

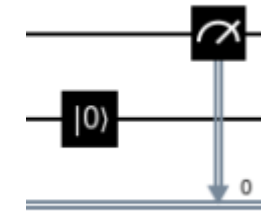
# Potential Noisy Gates Library Improvements



**Add unit tests & error handling** for unsupported features (e.g. mid-circuit measurements).

**Support mid-circuit measurements** via:

- Projective sampling, or
- Circuit decomposition into sequential cycles.



**Enable noisy reset gates** conditioned on measurement outcomes.

**Generalize noise models** to arbitrary Hamiltonians by automating symbolic variance & covariance derivations.

**Expand use cases** by integrating full surface code examples or other QEC schemes.

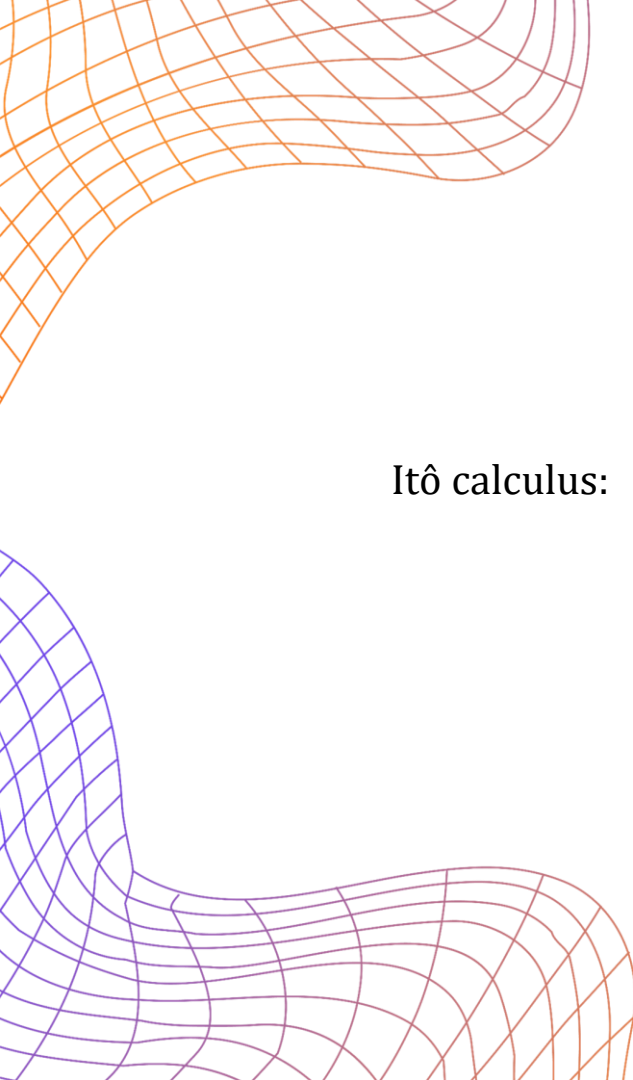


# Questions?

# References

1. A. G. Fowler , M. Mariantoni, J. M. Martinis, & A. N. Cleland (2012) *Surface codes: Towards practical large-scale quantum computation.* *Physical Review A*, vol. 86 no. 3, 032324. <https://doi.org/10.1103/PhysRevA.86.032324>
2. G. Di Bartolomeo, M. Vischi, F. Cesa, R. Wixinger, M. Grossi, S. Donadi, & A. Bassi, (2023) *Noisy gates for simulating quantum computers.* *Physical Review Research*, vol. 5 no. 4, 043210. <https://doi.org/10.1103/PhysRevResearch.5.043210>
3. E. National Academies of Sciences and Medicine, *Quantum Computing: Progress and Prospects*, Accessed: 2025-06-05, 2019. <https://www.ncbi.nlm.nih.gov/books/NBK538701/>
4. A. G. Fowler , D. Sank, J. Kelly, R. Barends, & J. M. Martinis, (2014) *Scalable extraction of error models from the output of error detection circuits.* *arXiv preprint arXiv:1405.1454.* <https://arxiv.org/abs/1405.1454>
5. D. Gottesman, (1997) *Stabilizer Codes and Quantum Error Correction.* PhD Thesis, Caltech. <https://arxiv.org/abs/quant-ph/9705052>
6. CERN IT Innovation (2025) *quantum-gates* [GitHub Repository]. <https://github.com/CERN-IT-INNOVATION/quantum-gates>
7. B. Gu, & I. Franco, (2019). *When can quantum decoherence be mimicked by classical noise?* *The Journal of Chemical Physics*, 151(1), 014109. <https://doi.org/10.1063/1.5099499>
8. D. C. McKay, C. J. Wood, S. Sheldon, J. M. Chow, & J. M. Gambetta, (2017) *Efficient Z-Gates for Quantum Computing.* *Physical Review A*, vol. 96 no. 2, 022330. <https://doi.org/10.1103/PhysRevA.96.022330>
9. Lao, Lingling & Wee, B & Ashraf, Imran & van Someren, Hans & Khammassi, Nader & Bertels, Koen & Almudever, C. (2018). Mapping of lattice surgery-based quantum circuits on surface code architectures. *Quantum Science and Technology*. 4. 10.1088/2058-9565/aadd1a.

# **EXTRA MATERIAL**



Let  $\{W_{k,s}\}_{k=1}^n$  denote a collection of independent Wiener processes (also known as standard Brownian motions), indexed by a discrete label  $k$  and continuous time  $s \geq 0$ . Each process  $W_{k,s} = W_k(s)$  satisfies:

1.  $W_{k,0} = 0$
2.  $W_{k,s}$  has continuous sample paths
3. The increments are independent and normally distributed:  
 $W_{k,s+\Delta s} - W_{k,s} \sim \mathcal{N}(0, \Delta s)$
4. The infinitesimal increment is denoted by  
 $dW_{k,s} := W_{k,s+ds} - W_{k,s}$

From 3. and 4. we can conclude  $dW_{k,s} := W_{k,s+ds} - W_{k,s} \sim \mathcal{N}(0, \Delta s)$

$$\mathbb{E}[dW_{k,s}] = 0, \quad \text{Var}[dW_{k,s}] = ds, \quad (77)$$

$$\mathbb{E}[dW_{k,s}^2] = \text{Var}[dW_{k,s}] + (\mathbb{E}[dW_{k,s}])^2 = ds \quad (78)$$

$$\mathbb{E}[dW_{k,s} dW_{k',s}] = \begin{cases} \mathbb{E}[dW_{k,s}] \mathbb{E}[dW_{k',s}], & \text{if } k \neq k', \\ \mathbb{E}[dW_{k,s}^2] = ds & \text{if } k = k' \end{cases} = \delta_{k,k'} ds \quad (79)$$

Eq. (79) signifies that for  $k \neq k'$ , the processes are independent  
 $\mathbb{E}[dW_{k,s} dW_{k',s}] = \delta_{kk'} ds$

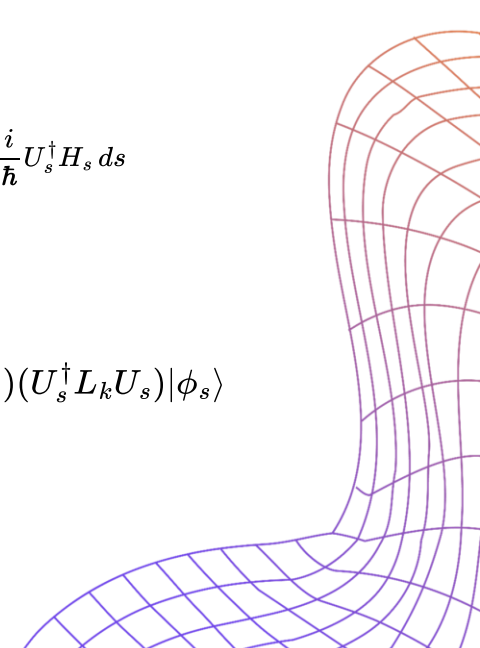
Another important identity is the Itô product rule:

$$d(XY) = dX \cdot Y + X \cdot dY + dX \cdot dY \quad (80)$$



$$L_{k,s} = L_k(s) = U_s^\dagger \sigma_k U_s$$

Itô stochastic differential equation in the interaction picture:



$$i\hbar \frac{dU_s}{ds} = H_s U_s$$

$$d|\psi_s\rangle = \left[ -\frac{i}{\hbar} H_s ds + \sum_k \left( i\epsilon L_k dW_{k,s} - \frac{\epsilon^2}{2} L_k^\dagger L_k ds \right) \right] |\psi_s\rangle$$

$$|\phi_s\rangle = U_s^\dagger |\psi_s\rangle \quad \text{where} \quad U_s = \mathcal{T} \exp \left( -\frac{i}{\hbar} \int_0^s H_\tau d\tau \right)$$

$$d|\phi_s\rangle = d(U_s^\dagger |\psi_s\rangle) = (dU_s^\dagger) |\psi_s\rangle + U_s^\dagger d|\psi_s\rangle$$

$$i\hbar \frac{dU_s}{ds} = H_s U_s \quad \Rightarrow \quad \frac{d}{ds} U_s = \frac{-i}{\hbar} H_s U_s \quad \Rightarrow \quad \frac{d}{ds} U_s^\dagger = \frac{i}{\hbar} U_s^\dagger H_s \quad \Rightarrow \quad dU_s^\dagger = \frac{i}{\hbar} U_s^\dagger H_s ds$$

$$d|\phi_s\rangle = \sum_k \left( i\epsilon dW_{k,s} U_s^\dagger L_k |\psi_s\rangle - \frac{\epsilon^2}{2} ds U_s^\dagger L_k^\dagger L_k |\psi_s\rangle \right)$$

$$|\psi_s\rangle = U_s |\phi_s\rangle \quad \Rightarrow \quad U_s^\dagger L_k |\psi_s\rangle = U_s^\dagger L_k U_s |\phi_s\rangle, \quad U_s^\dagger L_k^\dagger L_k |\psi_s\rangle = (U_s^\dagger L_k^\dagger U_s)(U_s^\dagger L_k U_s) |\phi_s\rangle$$

$$d|\phi_s\rangle = \left[ i\epsilon \sum_k dW_{k,s} L_{k,s} - \frac{\epsilon^2}{2} \sum_k ds L_{k,s}^\dagger L_{k,s} \right] |\phi_s\rangle.$$

## C. Explicit calculation of the depolarizing component

### C.1. Y Component

We consider the general  $U_s$  for a  $R_{xy}(\theta, \phi)$  rotation. Therefore, the conjugation of the Y Pauli operator is  $Y(s) = U_s^\dagger Y U_s$ :

$$U_s^\dagger Y U_s = \begin{pmatrix} -\sin(s\theta)\cos(\phi) & i(-\cos^2(\frac{s\theta}{2}) + e^{-2i\phi}\sin^2(\frac{s\theta}{2})) \\ i(\cos^2(\frac{s\theta}{2}) - e^{2i\phi}\sin^2(\frac{s\theta}{2})) & \sin(s\theta)\cos(\phi) \end{pmatrix} \quad (96)$$

Each of the components is found by applying:  $f_{i,s}^{(Y)} = \frac{1}{2}Tr[Y(s) \cdot \sigma_i]$

$$\begin{aligned} f_Y^{(z)}(s) &= \frac{1}{2}Tr[Y(s) \cdot \sigma_z] \\ &= \frac{1}{2}Tr \begin{pmatrix} -\sin(s\theta)\cos(\phi) & i(\cos^2(\frac{s\theta}{2}) - e^{-2i\phi}\sin^2(\frac{s\theta}{2})) \\ i(\cos^2(\frac{s\theta}{2}) - e^{2i\phi}\sin^2(\frac{s\theta}{2})) & -\sin(s\theta)\cos(\phi) \end{pmatrix} \\ &= -\sin(s\theta)\cos(\phi), \end{aligned} \quad (97)$$

$$f_Y^{(I)}(s) = \frac{1}{2}Tr[Y(s) \cdot \sigma_z] = 0, \quad (98)$$

$$f_Y^{(x)}(s) = \sin(2\phi) \cdot \sin^2(\frac{s\theta}{2}), \quad (99)$$

$$f_Y^{(y)}(s) = 1 + 2(1 - \sin^2(\phi)) \cdot \sin^2(\frac{s\theta}{2}) \quad (100)$$

From this we can compute  $\xi_Y^{(j)} := \int_0^1 f_Y^{(j)}(s)dW_{k,s}$ :

$$\xi_Y^{(I)} = 0, \quad (101)$$

$$\xi_Y^{(x)} = \sin(2\phi) \cdot \int_0^1 \sin^2(\frac{s\theta}{2})dW_{k,s} \quad (102)$$

$$\xi_Y^{(y)} = \int_0^1 1 \cdot dW_{k,s} + 2(1 - \sin^2(\phi)) \cdot \int_0^1 \sin^2(\frac{s\theta}{2})dW_{k,s}, \quad (103)$$

$$\xi_Y^{(z)} = -\cos(\phi) \cdot \int_0^1 \sin(s\theta)dW_{k,s} \quad (104)$$

This leaves us with three different integrals over  $dW_{k,s}$ .

$$I_Y^{(1)}(s) = \int_0^1 1 \cdot dW_{k,s}, \quad (105)$$

$$I_Y^{(2)}(s) = \int_0^1 \sin(s\theta)dW_{k,s}, \quad (106)$$

$$I_Y^{(3)}(s) = \int_0^1 \sin^2(\frac{s\theta}{2})dW_{k,s} \quad (107)$$

$$\rightarrow \xi_Y^{(I)} = 0, \quad \xi_Y^{(x)} = \sin(2\phi) \cdot I_Y^{(3)} \quad (108)$$

$$\rightarrow \xi_Y^{(y)} = I_Y^{(1)} + 2(1 - \sin^2(\phi))I_Y^{(3)}, \quad \xi_Y^{(z)} = -\cos(\phi)I_Y^{(2)} \quad (109)$$

Having defined  $\xi_Y^i$  for all  $i \in \{I, x, y, z\}$ , we can compute the Y-component of  $\Xi$  in Eq. (54):

$$\Xi_Y = i \epsilon_d \sum_{j=1}^3 \xi_Y^j \sigma_i = \begin{pmatrix} -\cos(\phi) \cdot I_Y^{(2)} & -i \cdot I_Y^{(1)} + \alpha_-(\phi) \cdot I_Y^{(3)} \\ i \cdot I_Y^{(1)} + \alpha_+(\phi) \cdot I_Y^{(3)} & \cos(\phi) \cdot I_Y^{(2)} \end{pmatrix} \quad (110)$$

with  $\alpha_{\pm} = [\sin(2\phi) \pm 2i(1 - \sin^2(\phi))] = \pm i(e^{\mp 2i\phi} + 1)$ .

The Itô-integrals (??) are sampled over the covariance matrix, computed as in Eq. (50). The covariance matrix for the Y component discussed here is as follows:

$$\Sigma = \begin{pmatrix} 0 & 0 & 0 \\ 0 & \frac{2\theta - \sin(2\theta)}{4\theta} & \frac{\sin^4(\theta/2)}{\theta} & \frac{1 - \cos(\theta)}{\theta} \\ 0 & \frac{\sin^4(\theta/2)}{\theta} & \frac{6\theta - 8\sin(\theta) + \sin(2\theta)}{\theta} & \frac{\theta}{\theta - \sin(\theta)} \\ 0 & \frac{\theta}{\theta} & \frac{16\theta}{2\theta} & 1 \end{pmatrix} \quad (111)$$

## D. Noise Extension to $R_{xyz}$

### Pauli Basis Components $f_X^{(j)}(s)$ for $R_{xyz}$ Rotation

$$f_Z^{(I)}(s) = 0$$

$$f_X^{(x)}(s) = \sin^2(\psi) \sin^2\left(\frac{s\theta}{2}\right) \cos(2\phi) - \sin^2\left(\frac{s\theta}{2}\right) \cos^2(\psi) + \cos^2\left(\frac{s\theta}{2}\right)$$

$$f_X^{(y)}(s) = \sin(2\phi) \sin^2(\psi) \sin^2\left(\frac{s\theta}{2}\right) - \sin(s\theta) \cos(\psi)$$

$$f_X^{(z)}(s) = 2 \left( \sin(\phi) \cos\left(\frac{s\theta}{2}\right) + \sin\left(\frac{s\theta}{2}\right) \cos(\phi) \cos(\psi) \right) \sin(\psi) \sin\left(\frac{s\theta}{2}\right)$$

### Pauli Basis Components $f_Y^{(j)}(s)$ for $R_{xyz}$ Rotation

$$f_Z^{(I)}(s) = 0$$

$$f_Y^{(x)}(s) = \sin(2\phi) \sin^2(\psi) \sin^2\left(\frac{s\theta}{2}\right) + \sin(s\theta) \cos(\psi)$$

$$f_Y^{(y)}(s) = -\sin^2(\psi) \sin^2\left(\frac{s\theta}{2}\right) \cos(2\phi) - \sin^2\left(\frac{s\theta}{2}\right) \cos^2(\psi) + \cos^2\left(\frac{s\theta}{2}\right)$$

$$f_Y^{(z)}(s) = 2 \left( \sin(\phi) \sin\left(\frac{s\theta}{2}\right) \cos(\psi) - \cos(\phi) \cos\left(\frac{s\theta}{2}\right) \right) \sin(\psi) \sin\left(\frac{s\theta}{2}\right)$$

### Pauli Basis Components $f_Z^{(j)}(s)$ for $R_{xyz}$ Rotation

$$f_Z^{(I)}(s) = 0$$

$$f_Z^{(x)}(s) = 2 \left( -\sin(\phi) \cos\left(\frac{s\theta}{2}\right) + \sin\left(\frac{s\theta}{2}\right) \cos(\phi) \cos(\psi) \right) \sin(\psi) \sin\left(\frac{s\theta}{2}\right)$$

$$f_Z^{(y)}(s) = 2 \left( \sin(\phi) \sin\left(\frac{s\theta}{2}\right) \cos(\psi) + \cos(\phi) \cos\left(\frac{s\theta}{2}\right) \right) \sin(\psi) \sin\left(\frac{s\theta}{2}\right)$$

$$f_Z^{(z)}(s) = -2 \sin^2(\psi) \sin^2\left(\frac{s\theta}{2}\right) + 1$$

Gate	$\theta$	$\psi$	$\phi$
$I$	$2\pi$	-	-
$X$	-	$\frac{\pi}{2}$	0
$Y$	-	$\frac{\pi}{2}$	$\frac{\pi}{2}$
$Z$	-	0	$\frac{\pi}{2}$

## D.1. Demonstrating Rotational Symmetry in the Noise Model

To illustrate the rotational symmetry of the depolarizing noise model, we examine the covariance matrices for noisy  $X$ ,  $Y$ , and  $Z$  gates, each evaluated in its respective dominant component. In the  $X$  component of the noisy  $X$  gate, the variance is exactly 1, while all other components vanish; the same holds for the  $Y$  component of the noisy  $Y$  gate and the  $Z$  component of the noisy  $Z$  gate. This yields the following covariance matrices:

$$\text{Cov}_X = \begin{pmatrix} 1 & 0 & 0 \\ 0 & 0 & 0 \\ 0 & 0 & 0 \end{pmatrix}, \quad \text{Cov}_Y = \begin{pmatrix} 0 & 0 & 0 \\ 0 & 1 & 0 \\ 0 & 0 & 0 \end{pmatrix}, \quad \text{Cov}_Z = \begin{pmatrix} 0 & 0 & 0 \\ 0 & 0 & 0 \\ 0 & 0 & 1 \end{pmatrix}$$

These matrices clearly show that the noise distribution is symmetric under coordinate rotation: each principal axis is treated identically under depolarization.

In contrast the covariance matrices for the other directions (i.e., projecting a noisy  $X$  gate onto  $Y$  or  $Z$ , etc.) contain non-trivial trigonometric structures of  $\theta$ . Below we list the corresponding Hermitian covariance matrices for the noisy  $Y$  gate when evaluated in the  $X$  and  $Z$  components.

$$\Sigma_Y^{(x)} = \begin{pmatrix} \frac{2\theta + \sin(2\theta)}{4\theta} & 0 & \frac{\sin^2(\theta)}{2\theta} \\ 0 & 0 & 0 \\ \frac{\sin^2(\theta)}{2\theta} & 0 & \frac{2\theta - \sin(2\theta)}{4\theta} \end{pmatrix}, \quad \Sigma_Y^{(z)} = \begin{pmatrix} \frac{2\theta - \sin(2\theta)}{4\theta} & 0 & \frac{\sin^2(\theta)}{2\theta} \\ 0 & 0 & 0 \\ \frac{\sin^2(\theta)}{2\theta} & 0 & \frac{2\theta + \sin(2\theta)}{4\theta} \end{pmatrix} \quad (119)$$

These matrices also exhibit a structural symmetry: the diagonal entries are symmetric combinations of  $2\theta \pm \sin(2\theta)$ , and the off-diagonal covariances involve  $\sin^2(\theta)$ , always scaled by  $\theta$ . This indicates that the model remains rotationally symmetric in structure.